JOC The Journal of Organic Chemistry

Article

pubs.acs.org/joc

Self-Sensitized Photooxygenation of 2*H*-Pyrans: Characterization of Unexpected Products Assisted by Computed Structural Elucidation and Residual Dipolar Couplings

Martín J. Riveira,[†] Pablo Trigo-Mouriño,[‡] Eduardo Troche-Pesqueira,[‡,§] Gary E. Martin,[∥] Armando Navarro-Vázquez,[⊥] Mirta P. Mischne,*[,†] and Roberto R. Gil*[,‡]

[†]Instituto de Química Rosario, Facultad de Ciencias Bioquímicas y Farmacéuticas, Universidad Nacional de Rosario-CONICET, Suipacha 531, S2002LRK Rosario, Argentina

[‡]Department of Chemistry, Carnegie Mellon University, Pittsburgh, Pennsylvania 15213, United States

[§]Departamento de Química Orgánica, Edificio de Ciencias Experimentais, Universidade de Vigo, Campus Universitario, 36310 Vigo, Spain

[∥]NMR Structure Elucidation, Process & Analytical Chemistry, Merck Research Laboratories, Rahway, New Jersey 07065, United States

[⊥]Departamento de Química Fundamental, Universidade Federal de Pernambuco, Cidade Universitária, CEP 50.740-540 Recife, Pernambuco, Brazil

Supporting Information

ABSTRACT: The UVA (350 nm) irradiation of an α-pyran in the presence of oxygen led to the unexpected formation of a tetraoxygenated compound whose structure could not be unambiguously determined on the basis of conventional $^{1}H-^{13}C$ correlated experiments. 1,1-ADEQUATE (adequate double quantum transfer experiment) and 1,*n*-ADEQUATE combined with computer-assisted structure elucidation software led to two structural possibilities involving the formation of either an epoxide or an oxetane. Residual dipolar couplings allowed not only the identification of the compound as a spiroepoxide but also the determination of its relative configuration. To account for its formation, we propose a bisepoxide intermediate that, as opposed to most α,β-epoxyketones under irradiation, undergoes $O-C_{\beta}$ cleavage probably due to the presence of an extra oxygen substituent in the β position. 1,2-Acyl migration would then proceed stereoselectively to the final product obtained as a single diastereomer.

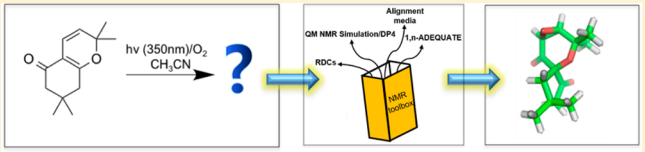

INTRODUCTION

The oxidation of organic compounds using molecular oxygen as an oxidizing agent is an active area of research. Conjugated dienes, polyenes, and heterocyclic systems are substrates of particular interest due to their ability to incorporate peroxide linkages, leading to highly oxygenated products which, in some cases, can undergo further chemical transformations providing unique molecular architectures in one-pot sequences.[1] Generally, singlet oxygen is the reagent of choice in these processes, requiring the use of an external sensitizer for the energy transfer process to occur.[2−5] During our studies on the photochemical behavior of dienones in the presence of molecular oxygen, we established an easy one-pot approach for the preparation of bridged 1,2,4-trioxanes (Scheme 1).[6−8] The process involves a singlet oxygen Diels−Alder-type oxygenation of 2*H*-pyran intermediates generated *in situ*, revealing the ability of dienones bearing an ionone-type skeleton to act as singlet oxygen sensitizers.

Dienones and 2*H*-pyrans are well-known valence isomers that can interconvert through an oxa-6π-electrocyclic reaction, and this equilibrium has been the focus of extensive research for diverse applications.[9] In many cases, the Knoevenagel-type condensation between 1,3-dicarbonyl substrates and α,β-unsaturated aldehydes has been shown to afford 2*H*-pyran derivatives exclusively, suggesting a complete shift toward the ring-closed form presumably due to either steric destabilization or the absence of stabilizing mesomeric effects in the open form of the conjugated dienone.[10] To test whether 2*H*-pyrans can also undergo self-sensitized photooxygenation toward 1,2,4-trioxanes, we attempted the irradiation of 2*H*-pyran **1**, prepared

Scheme 1. Self-Sensitized Photooxygenation of β-Ionone Derivatives

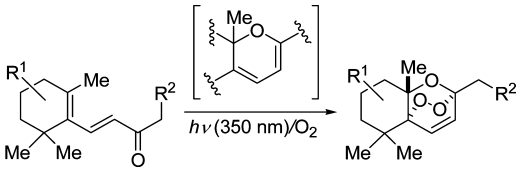

Received: April 13, 2015
Published: June 10, 2015

DOI: 10.1021/acs.joc.5b00817
J. Org. Chem. 2015, 80, 7396−7402

via Knoevenagel condensation between dimedone and 3-methylcrotonaldehyde,[11] in the presence of oxygen (Scheme 2). Mindful of the photochemical behavior of ionone-type

Scheme 2. Attempted Photooxygenation of 2*H*-Pyran 1

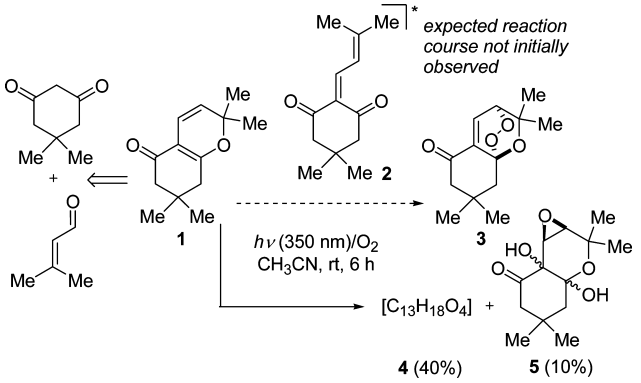

compounds, we envisioned that upon irradiation valence isomer equilibrium would switch the 2*H*-pyran cyclized form **1** toward the dienone open form **2**, which could then sensitize singlet oxygen formation required for the putative [4 + 2] cycloaddition toward peroxide **3**. After 6 h of irradiation, ^{1}H NMR monitoring indicated complete consumption of 2*H*-pyran **1**. To our surprise, the absence of olefinic signals indicated that the expected 1,2,4-trioxane **3** had not been formed as a product of the reaction. After purification, unexpected product **4** along with an inseparable mixture of two diastereomeric epoxydiols (**5**) could be isolated. Herein we report our efforts to elucidate the challenging structure of the major product of the reaction as well as propose a feasible mechanistic pathway for this unprecedented photochemical tandem process.

RESULTS AND DISCUSSION

The high-resolution positive ion ESI-MS spectrum of the unexpected product (main product **4**, 40% yield) revealed a molecular formula of $C_{13}H_{18}O_4$ based on a pseudomolecular ion $[M + H]^+$ at m/z 239.1277 (calcd 239.1278 for $C_{13}H_{19}O_4$). Hence, two more oxygen atoms are incorporated into compound **1** during the oxidation process without altering the number of carbon and hydrogen atoms in the molecule. The ^{1}H NMR spectrum of **4** exhibits an AB system with doublets centered at 3.47 and 3.45 ppm (J_{AB} = 4.5 Hz), and no vinyl protons, suggesting an epoxidation of the disubstituted double bond. The spectrum also features four sharp singlets at 1.43, 1.40, 1.15, and 1.12 ppm corresponding to CH_3 groups, and two additional AB systems between 2.40 and 2.00 ppm corresponding to two CH_2 groups (see the Experimental Section and Figure S1, Supporting Information). In addition, the combined analysis of the 1D ^{13}C NMR, multiplicity-edited HSQC, and HMBC spectra suggests that the fragments highlighted in Scheme 3 for structure **1** are conserved in the structure of **4**.

The ^{13}C NMR spectrum of **4** shows the presence of two carbonyl groups at δ = 212.2 and 204.7 ppm. Considering the epoxidation leading to a structure like **A**, we initially thought of **B** as the possible planar structure for compound **4** after incorporation of the second carbonyl group. One of the major limitations of the HMBC experiments is that it is not possible to unambiguously differentiate two-bond from three-bond heteronuclear correlations, and this problem gets considerably

Scheme 3. Conserved Fragments and Possible Reaction Products

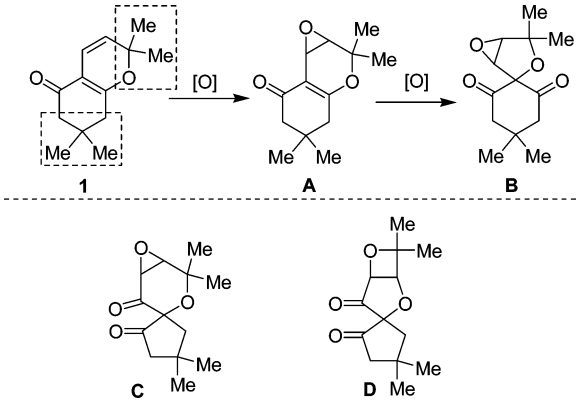

worse in compact structures such as **4** (**B**), in which most of the carbons are located no further than two to three bonds away from most of the protons. As a consequence, apart from **B**, structures **C** and **D** can also satisfy the experimental data provided by a conventional data set of NMR experiments (1D ^{1}H, 1D ^{13}C, HSQC, and HMBC). These limitations can be lifted if carbon−carbon correlation information is available through INADEQUATE-type[12] or ADEQUATE-type[13−15] experiments (INADEQUATE = incredible natural abundance double quantum transfer experiment; ADEQUATE = adequate double quantum transfer experiment). The ^{13}C-observed INADEQUATE is an extremely powerful NMR experiment for establishing a molecular framework but has severe sensitivity limitations and prodigious sample requirements. In contrast, the ^{1}H-observed 1,1-ADEQUATE has roughly 32 times the sensitivity of the INADEQUATE experiment and provides most of the same carbon−carbon connectivity information with the exception of correlations between adjacent nonprotonated carbons. The 1,*n*-ADEQUATE experiment provides long-range carbon−carbon correlations, most frequently via $^3J_{CC}$, which are complementary to the HMBC data.[16,17]

In our case, sample availability was not a problem, and 1,1- as well as 1,*n*-ADEQUATE 2D NMR data were acquired using a solution of 50 mg of **4** in 500 μL of $CDCl_3$. A useful presentation of the 1,1- and/or 1,*n*-ADEQUATE data that facilitates interpretation is obtained by mathematically combining the ADEQUATE data with an identically digitized, unedited HSQC spectrum using either unsymmetrical (UIC)[18] or generalized (GIC)[19] indirect covariance processing. The HSQC-1,1-ADEQUATE plot generated in the calculation from the 1,1-ADEQUATE data will exhibit diagonally symmetric correlations between adjacent protonated carbons (C3 and C4 for **4**), and for correlations between protonated and adjacent nonprotonated carbons, the plot will contain diagonally asymmetric correlations at the F1 shift of the nonprotonated carbon and the F2 frequency of the protonated carbon. The annotated HSQC-1,1-ADEQUATE spectrum of **4** is presented in Figure 1.[16,17]

The 1,1-ADEQUATE experiment (Figure 1; Figure S5, Supporting Information) has clearly shown a series of key carbon−carbon correlations, such as (a) one of the putative epoxide carbons (53.7) is connected to one of the carbonyl carbons (204.7), while the other epoxide carbon (63.3) is directly connected to a quaternary carbon at 71.4 ppm, and (b)

DOI: 10.1021/acs.joc.5b00817
J. Org. Chem. 2015, 80, 7396−7402

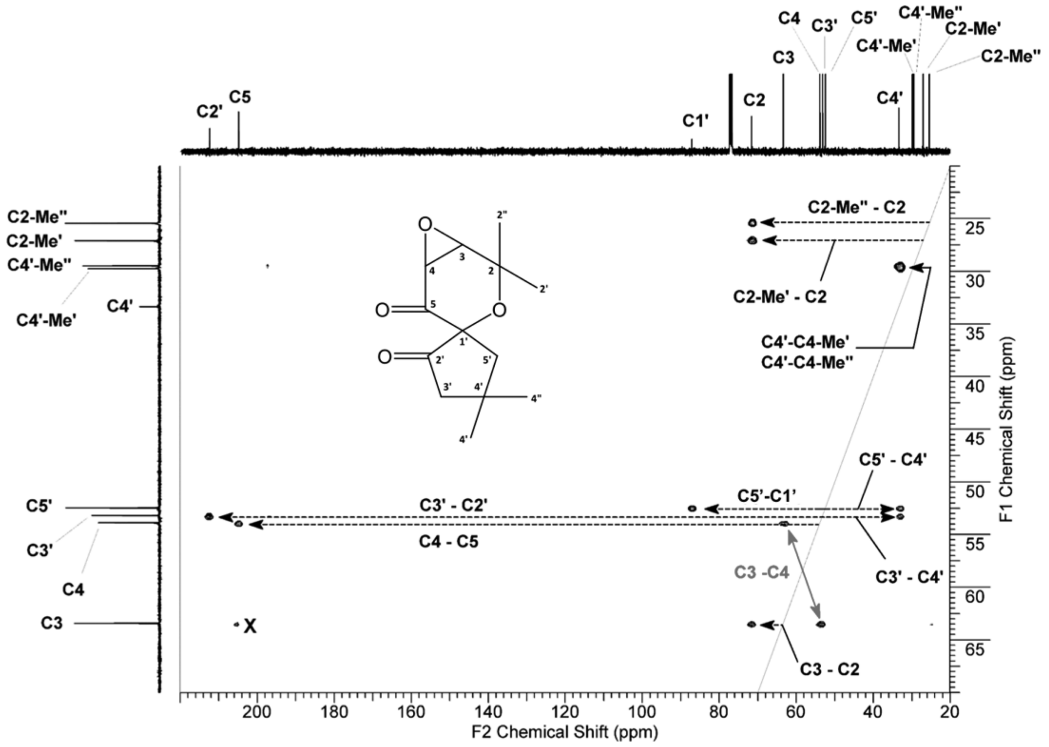

Figure 1. Covariance-calculated HSQC-1,1 ADEQUATE plot. The cross-peak marked with an "X" is a covariance calculation artifact from a tailing to the left in the F2 dimension of the 1,1-ADEQUATE cross-peak between C5 and C3.

one of the CH_2 carbons is connected to the quaternary carbon at 87.0 ppm, while the other CH_2 carbon is connected to the other carbonyl carbon at 212.2 ppm. These data are satisfied if one of the carbonyl groups is moved from the six-membered ring in structure **B** and is located between the epoxide group and the spiro center as in structure **C** (Scheme 3). To not miss any compatible structure, we decided to feed the available data to a computer-assisted structure elucidation (CASE) program. When the 1D ^{1}H, 1D ^{13}C, HSQC, HMBC, 1,1-ADEQUATE, and 1,*n*-ADEQUATE NMR experimental data were passed to the structure elucidator program ADCLabs,[20] another compatible structure (**D**) was also generated (see Scheme 3). At this point, the molecular constitution of **4** has still not been unambiguously determined, and presumably structure **C** or **D** could be correct. It is important to highlight that structure **D** was not obvious to us during the manual analysis of the NMR data, including the ADEQUATE-type experiments. However, when the $^{1}J_{CH}$ couplings of the two carbons tentatively attributed to the epoxide moiety are considered, structure **D** can be ruled out as follows. By examining the HMBC spectrum for residual, incompletely canceled $^{1}J_{CH}$ doublets, the putative epoxide carbons had one-bond couplings of 181.2 and 190.5 Hz for the carbons assigned as C3 and C4, respectively. When the $^{1}J_{CH}$ coupling constants for C3 and C4 of the epoxide and oxetane were calculated by DFT methods, the epoxide carbons gave calculated $^{1}J_{CH}$ couplings of 181.1 and 188.3 Hz, respectively. In contrast, as expected, the C3 and C4 carbons of the oxetane ring were 159.8 and 164.6 Hz, respectively. This constitutional assignment was also supported by chemical shift and residual dipolar coupling analyses. In recent years additional techniques such as DFT calculations and residual dipolar couplings (RDCs) have become a part of the NMR toolbox for challenging structure elucidation problems. The use of DFT-based chemical shift predictions has been shown to be a powerful tool for the determination of chemical constitution.[21] Residual dipolar coupling analysis has also been recently applied to the determination of chemical constitution.[22] RDC analysis normally comprises the extraction of scalar $^{1}J_{CH}$ couplings from isotropic samples and total $^{1}T_{CH}$ couplings ($^{1}T_{CH} = {}^{1}J_{CH} + {}^{1}D_{CH}$) from samples in which a small degree of alignment has been introduced, in such a way that, by subtracting the scalar couplings ($^{1}J_{CH}$) from the total coupling, a set of RDCs ($^{1}D_{CH}$) can be obtained for every CH pair. This set of RDCs is then fitted to the molecular coordinates of the given molecules, and an alignment tensor accounting for the rotational distribution of the molecule is then obtained. The congruence of the fit between the theoretical RDCs extracted from the alignment tensor of each molecule with respect to the experimental set of values allows the correct structure to be selected.[23,24] Note that NOE-based experiments would not help in solving the epoxide/oxetane problem in this case, since protons from the bridge and the two methyl groups would be expected to show cross-peaks in both scenarios. Having this in mind, RDCs were the *go to* option. The choice of the alignment media employed was not a trivial matter either.[25] There are mainly two options: cross-linked polymers or homopolypeptides. The differences between both types of alignment media are vast, with cross-linked polymers generally presenting a more user-friendly sample preparation, better shimming homogeneity, smaller influence on the T_2 relaxation time of the sample, and a degree of alignment more suitable for regular- to small-sized organic molecules. Due to the very small size and also overall oval shape of this molecule, attempts to align it in PMMA[26] and PDMS[27] gels swollen with $CDCl_3$ failed, producing very small RDCs on the order of the experimental error. Hence, we decided to use a lyotropic liquid crystalline solution of poly(γ-ethyl-L-glutamate) (PELG) in $CDCl_3$, as first reported by Aroulanda et al.,[28] because of its stronger aligning

DOI: 10.1021/acs.joc.5b00817
J. Org. Chem. 2015, 80, 7396−7402

properties. RDCs were measured using the *J*-scaled F1 proton-coupled bilinear rotation decoupling HSQC (JSBHSQC) experiment.[29,30]

By inverting the configuration of the spiro carbon atom, two diastereomers were generated for the epoxide **4** (**C**) (e*RSR* and e*RSS*) and oxetane **4** (**D**) (o*RRR* and o*RRS*) structures (Figure 2). Conformational search using molecular mechanics followed

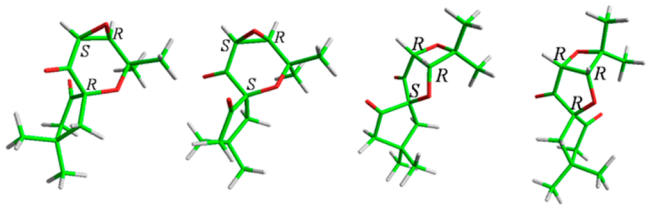

Figure 2. Possible epoxide **4** (**C**) and oxetane **4** (**D**) diastereomers.

by DFT energy minimization and frequency calculation yielded two possible conformations per diastereoisomer. Their relative populations were calculated on the basis of the relative Gibbs free energies using the Boltzmann equation.

Singular value decomposition (SVD)[31] fitting of the RDC data to the DFT-optimized structures was accomplished using the MSpin program.[32] The presence of two conformations per diastereoisomer was taken into account by using the single-tensor approximation;[33] i.e., a common alignment tensor is assumed for the different conformations of the molecule. The fit clearly and straightforwardly determined the constitution by selecting the epoxide structure over the oxetane (Table 1). The

Table 1. Relative Energies and Populations of the Conformers of Each Diastereoisomer of Epoxide 4 (C) and Oxetane 4 (D)

structure	E_{rel} (kcal/mol)	population	Q factor
e*RSR*_1	0	83	0.030
e*RSR*_2	1.06	17	
e*RSS*_1	0	97	0.066
e*RSS*_2	2.10	3	
o*RRR*_1	0	91	0.462
o*RRR*_2	1.41	9	
o*RRS*_1	0	93	0.258
o*RRS*_2	1.60	7	

quality of the fitting of the RDC data to the structure was evaluated using the Cornilescu quality factor (*Q*).[34] The lower the *Q*, the better the fitting; values of 0.030 for e*RSR* and 0.066 for e*RSS*, compared to 0.462 for o*RRR* and 0.258 for o*RRS* were obtained, clearly showing a very poor fitting for the oxetane structures.

The constitution of **4** and its relative configuration of the epoxide was independently confirmed by using the DP4 probability method developed by Goodman and co-workers,[35] which is based on ^{1}H and ^{13}C DFT GIAO NMR chemical shift calculations. On the basis of previous database computations, the DP4 method translates the matching of experimental vs computed values to a single probability value, and it has been used successfully in our group for cross-validation RDC results.[36,37] The weighted population averaged ^{1}H, ^{13}C, and ^{13}C + ^{1}H chemical shifts were calculated for each structure and compared with the experimental values using the aforementioned DP4 method, giving a 100% probability for the ensemble of the epoxide e*RSR*, the isomer also selected by RDCs (Table 2).

Table 2. DP4 Probabilities (%) for the Weighted Conformational Ensembles of Diastereoisomers of Epoxide 4 (C) and Oxetane 4 (D)

	^{1}H	^{13}C	^{13}C + ^{1}H
e*RSR*	97.8	99.3	100
e*RSS*	0.0	0.7	0
o*RRR*	0.8	0	0
o*RRS*	1.4	0	0

Once the structure of compound **4** was established, we turned our attention to devising a reasonable mechanistic explanation that could account for its formation. Two proposals are depicted in Schemes 4 and 5.

The first scenario involves an initial dioxetane formation as a result of a [2 + 2] cycloaddition between the tetrasubstituted double bond and *in situ* generated singlet oxygen (Scheme 4).

Scheme 4. First Mechanistic Proposal Involving a Dioxetane Intermediate

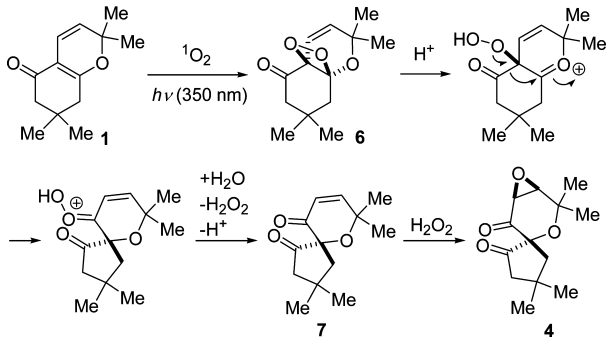

This dioxetane intermediate (**6**) could then undergo a rearrangement featuring a ring contraction that would yield the enone intermediate **7** after hydrogen peroxide release. Enone **7** could be eventually stereoselectively epoxidized with *in situ* formed hydrogen peroxide, giving rise to product **4**.

A second mechanistic proposal involves initial formation of originally sought 1,2,4-trioxane **3** (Scheme 5). Homolytic cleavage of the peroxide bridge in **3** would yield a biradical intermediate that could lead to bisepoxide **8**, a rearrangement that is known to occur in 1,2-dioxines.[38] Promoted by the presence of an extra oxygen substituent in the β position, α,β-epoxyketone **8** could then suffer O−C_β cleavage of the epoxide moiety, instead of the more common O−C_α cleavage,[39,40] leading to a zwitterionic intermediate (**9**) which, after a stereoselective [1,2]-acyl shift, would lead to the final product **4**. Instead, if this intermediate **9** is trapped by water, a mixture of epoxydiols could then result, which accounts for the two diastereomers found as byproducts (**5**).[41] Remarkably, the intermediacy of radical species, as proposed to result from peroxide bond cleavage, is supported by the fact that this reaction was significantly hampered by the addition of radical scavengers. For instance, using 2*H*-pyran analogue **10** as substrate, a 3-fold decrease in yield of spirocycle formation ensued when irradiation was carried out in the presence of hydroquinone (Scheme 6).

At this point, although this second mechanistic proposal seemed settled, further experimentation was conducted with

DOI: 10.1021/acs.joc.5b00817
J. Org. Chem. 2015, 80, 7396−7402

Scheme 5. Second Mechanistic Proposal Involving 1,2,4-Trioxane 3

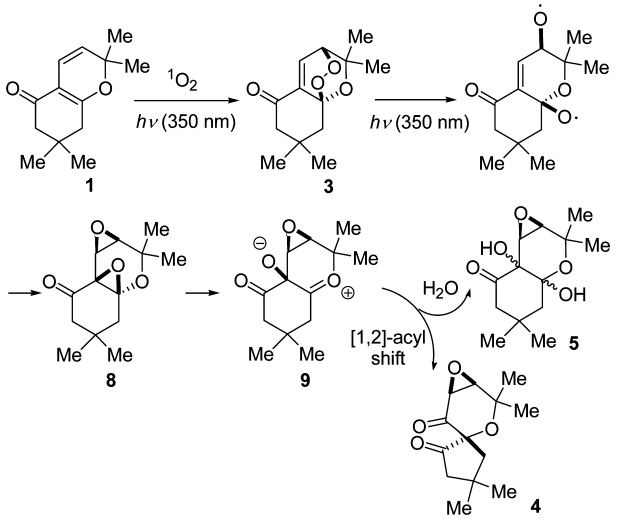

Scheme 6. Photooxygenation of 2*H*-Pyran 10 and Inhibitory Effect of Hydroquinone (HQ)

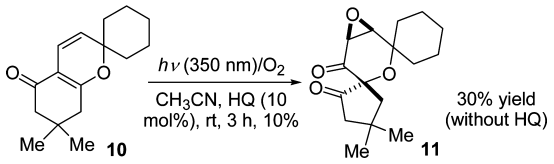

substrate **1**. To find any of the proposed intermediates, namely, trioxane **3** and bisepoxide **8**, the reaction was interrupted before complete consumption of starting material. To our delight, the originally sought trioxane **3** could be isolated in low yield (4%) in the reaction mixture (Scheme 7). Its structure was confirmed

Scheme 7. Isolation of Intermediate 1,2,4-Trioxane 3 and Its Rearrangement under UV Irradiation

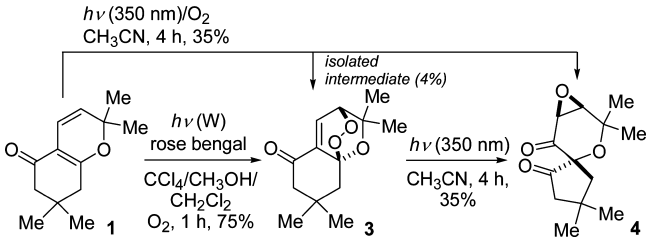

by comparison of spectral data with a sample synthesized by well-known dye-sensitized photooxygenation of **1**.[2,3] To validate that trioxane **3** is an intermediate toward **4** and not just a side product, it was irradiated under the same conditions as **1**, but without the bubbling of oxygen, to find that it produces **4** in almost exactly the same yield as **1**. It is clear then that this particular peroxidic scaffold is not stable under UVA irradiation, unlike the ionone-derived series.

In summary, an unprecedented domino photochemical transformation was uncovered which comprises the oxidation of 2*H*-pyrans toward spirocyclic systems. Structure elucidation was possible thanks to the combined applications of $^{13}C-^{13}C$ correlation experiments, computer-assisted structure elucidation, molecular modeling, DFT chemical shift prediction (DP4), and RDCs. Considering that spirocyclic compounds abound in nature and that there is an increased use of these scaffolds in drug discovery programs,[42,43] investigations to explore the potential of this synthetic methodology are under way.

EXPERIMENTAL SECTION

General Experimental Methods. Unsaturated precursor **1** has been previously prepared by our group.[11] Substrate **10** was prepared according to the same literature precedent. Dicarbonyl compound dimedone (140 mg, 1 mmol) and cyclohexylideneacetaldehyde[44] (124 mg, 1 mmol) were added to a mortar. After addition of the catalyst (ethylenediammonium diacetate, 18 mg, 0.1 mmol), the mixture was ground by pestle at room temperature for 5 min. The residue was then purified by column chromatography (SiO_2; hexanes/ethyl acetate, 9:1, v/v) to afford the desired compound **10** as a pale yellow solid in 70% yield (172 mg, 0.7 mmol). Mp: 69.5−70.0 °C. IR (KBr): 2939, 2909, 1639, 1591, 1420, 1231, 1136 cm^{-1}. ^1H NMR (300 MHz, $CDCl_3$, 300 K, TMS): δ 6.41 (d, J = 10.0 Hz, 1H), 5.27 (d, J = 10.0 Hz, 1H), 2.30 (br s, 2H), 2.25 (br s, 2H), 1.95−1.80 (m, 2H), 1.77−1.28 (m, 8H), 1.07 (s, 6H). ^{13}C NMR (75 MHz, $CDCl_3$, 300 K): δ 194.3 (C), 170.1 (C), 121.9 (CH), 116.1 (CH), 110.1 (C), 80.5 (C), 50.3 (CH_2), 42.2 (CH_2), 36.2 (2 × CH_2), 32.1 (C), 28.3 (2 × CH_3), 24.9 (CH_2), 20,8 (2 × CH_2). HRMS (ESI): m/z calcd for $C_{16}H_{22}NaO_2$ $[M+ Na]^+$ 269.1512, found 269.1507.

Most of the NMR spectra (1D ^1H, 1D ^{13}C, 1D ^{13}C DEPT, COSY, ROESY, HSQC, and HMBC) for compounds **3**, **4**, and **5** were collected at 300 K in an NMR instrument operating at 300.13 MHz for ^1H and 75 MHz for ^{13}C, using $CDCl_3$ as the solvent. Full ^1H and ^{13}C NMR assignment was performed for these compounds using a combination of 1D and 2D NMR data, and the assignments are annotated on the spectra provided in the Supporting Information. Chemical shifts are reported in parts per million relative to TMS (internal standard) for ^1H, and to the $CDCl_3$ carbon triplet (77.00 ppm) for ^{13}C. Coupling constants (J) are reported in hertz. The following abbreviations are used to indicate the multiplicities: s = singlet, d = doublet, t = triplet, q = quartet, m = multiplet, br = broad signal. JBSHSQC and ADEQUATE spectra of compound **4** were collected at 300 K on a two-channel NMR instrument operating at a frequency of 500.13 MHz for ^1H and 125.76 MHz for ^{13}C. 1,1- and 1,*n*-ADEQUATE 2D spectra were acquired as a 2048* (^{13}C) × 128* (^1H) data matrix, where *N** refers to *N* complex pairs, with acquisition times of 2.3 ms (^{13}C) and 204.8 ms (^1H), using a 5 s delay between scans. An isotropic 2D JBSHSQC spectrum was acquired as a 1024* (^{13}C) × 998* (^1H) data matrix, with acquisition times of 25.4 ms (^{13}C) and 99.8 ms (^1H), using a 1.5 s delay between scans. An anisotropic 2D JBSHSQC spectrum was acquired as a 256* (^{13}C) × 998* (^1H) data matrix, with acquisition times of 12.7 ms (^{13}C) and 99.8 ms (^1H), using a 1.5 s delay between scans. The shorter T_2 values observed for compound **4** in the PELG LLC solution did not justify the collection of 1024 increments in F1. In both JBSHSQC spectra, a J scaling factor of 4 was used.

A solution of 85 mg of PELG was prepared on 600 μL of $CDCl_3$, which already contained the sample under study, and a capillary tube with DMSO-d_6 was used to fix the lock signal. A strong alignment was obtained in this medium, with a deuterium quadrupolar splitting of 603 Hz for the chloroform signal. Both isotropic and anisotropic samples carried 15 mg of the sample under study.

Conformational searches were performed using the MMFF94 force field[45,46] in Macromodel[47] with a 5 kcal/mol energy window, a chloroform solvent model, and a dielectric constant of 1.0, taking the electrical charges from the parameters of the force field, and using the mixed torsional/low-mode sampling method. All of the structures were refined with Gaussian09[48] at the OPBE[49]/6-31G* level of theory in the gas phase, and vibrational frequencies were computed to check that all obtained stationary points were true minima. Solvation was taken into account using the polarizable continuum model (IEFPCM[50]) with chloroform Gaussian09 parameters. RDC fittings were performed using the MSpin[32] program, and the results were analyzed in terms of the Cornilescu quality factor.[34] NMR shielding tensors were obtained

DOI: 10.1021/acs.joc.5b00817
J. Org. Chem. 2015, 80, 7396−7402

at the PBE0[51]/pcS-2[52] level of theory. The computed shieldings were referenced to TMS and Boltzmann averaged (298 K) using the computed relative energies. To transform computed shieldings into chemical shifts, the reference shielding was obtained by minimizing the difference between experimental and computed data in a least-squares sense.

Self-Sensitized Photooxygenation of 1. The irradiation was performed at λ = 350 nm, in a photochemical reactor, in which a transparent glass vessel containing a 0.01 M solution of compound **1** (300 mg, 1.46 mmol) in CH_3CN (146 mL) was placed. A stream of oxygen was bubbled through the solution at room temperature. After 6 h, the solvent was removed under reduced pressure to afford a pale yellow residue that was purified by column chromatography (SiO_2; hexanes/ethyl acetate, 9.5:0.5, v/v) to give **4** as a colorless solid (139 mg, 40% yield) and **5** as a colorless oil (37 mg, 10% yield). The following are data for **4**. Mp: 52.0−52.5 °C. IR (KBr): 2987, 2972, 2960, 1755, 1708, 1466, 1368, 1168, 1022 cm^{-1}. ^1H NMR (300 MHz, $CDCl_3$, 300 K, TMS): δ 3.47 (d, J = 4.5 Hz, 1H, 3-H), 3.45 (d, J = 4.5 Hz, 1H, 4-H), 2.34 (dd, J = 17.6, 2.0 Hz, 1H, 3′-H), 2.25 (d, J = 17.6 Hz, 1H, 3′-H), 2.15 (dd, J = 14.3, 2.0 Hz, 1H, 5′-H), 2.09 (d, J = 14.3 Hz, 1H, 5′-H), 1.43 (s, 3H, 2-CH_3), 1.40 (s, 3H, 2-CH_3), 1.15 (s, 3H, 4′-CH_3), 1.12 (s, 3H, 4′-CH_3). ^{13}C NMR (75 MHz, $CDCl_3$, 300 K): δ 212.2 (C, C-2′), 204.7 (C, C-5), 87.0 (C, C-1′), 71.4 (C, C-2), 63.3 (CH, C-3), 53.7 (CH, C-4), 53.0 (CH_2, C-3′), 52.3 (CH_2, C-5′), 33.2 (C, C-4′), 29.6 (CH_3, C4′-CH_3), 29.3 (CH_3, C4′-CH_3), 26.9 (CH_3, C2-CH_3), 25.3 (CH_3, C2-CH_3). HRMS (ESI): m/z calcd for $C_{13}H_{19}O_4$ $[M + H]^+$ 239.1278, found 239.1277. The following are data for **5**. IR (film): 3433, 2959, 2628, 1720, 1049 cm^{-1}. ^1H NMR (300 MHz, $CDCl_3$, 300 K, TMS): δ 5.01 (br s, 1H), 4.49 (br s, 1H), 3.79 (d, J = 4.7 Hz, 1H), 3.77 (d, J = 2.9 Hz, 1H), 3.48 (d, J = 4.7 Hz, 1H), 3.32 (br s, 1H), 3.20 (d, J = 4.1 Hz, 1H), 3.14 (d, J = 4.2 Hz, 1H), 3.05 (d, J = 12.1 Hz, 1H), 2.83 (d, J = 12.6 Hz, 1H), 2.41 (dd, J = 14.0, 2.9 Hz, 1H), 2.34 (dd, J = 12.4, 2.6 Hz, 1H), 1.99 (d, J = 14.4 Hz, 1H), 1.97 (dd, J = 12.2, 2.1 Hz, 1H), 1.77 (dd, J = 14.2, 2.5 Hz, 1H), 1.65 (dd, J = 14.5, 2.0 Hz, 1H), 1.47 (s, 3H), 1.44 (s, 3H), 1.42 (s, 3H), 1.29 (s, 3H), 1.12 (s, 3H), 1.06 (s, 3H), 0.95 (s, 3H), 0.94 (s, 3H). ^{13}C NMR (75 MHz, $CDCl_3$, 300 K): δ 209.0 (C), 208.5 (C), 101.2 (C), 98.3 (C), 75.7 (C), 72.8 (C), 71.8 (C), 71.6 (C), 62.4 (CH), 58.4 (CH), 56.7 (CH), 55.0 (CH), 50.2 (CH_2), 48.7 (CH_2), 46.8 (CH_2), 45.0 (CH_2), 33.2 (CH_3), 32.8 (C), 32.7 (CH_3), 27.9 (CH_3), 27.4 (CH_3, CH_3), 27.0 (2 × CH_3), 26.2 (CH_3). HRMS (ESI): m/z calcd for $C_{13}H_{20}NaO_5$ $[M + Na]^+$ 279.1203, found 279.1197.

Compound 11. **11** was obtained as a pale yellow solid in 30% yield (100 mg, 0.36 mmol) using the same photooxygenation protocol and substrate **10** (300 mg, 1.2 mmol). Mp: 71.5−72.0 °C. IR (KBr): 2957, 2936, 2860, 1755, 1703, 1080 cm^{-1}. ^1H NMR (300 MHz, $CDCl_3$, 300 K, TMS): δ 3.46 (d, J = 4.5 Hz, 1H), 3.44 (d, J = 4.5 Hz, 1H), 2.38 (dd, J = 17.9 Hz, J = 2.3 Hz, 1H), 2.22 (overlapping d, J = 17.9 Hz, 1H), 2,18 (overlapping dd, J = 14.2 Hz, J = 2.4 Hz, 1H), 2.06 (d, J = 14.2 Hz, 1H), 2.00−1.81 (m, 2H), 1.69−1.41 (m, 7H), 1.34−1.22 (m, 1H), 1.21 (s, 3H), 1.14 (s, 3H). ^{13}C NMR (75 MHz, $CDCl_3$, 300 K): δ 212.1 (C), 205.1 (C), 87.0 (C), 72.4 (C), 63.1 (CH), 53.4 (CH_2), 53.2 (CH_2), 52.8 (CH), 35.9 (CH_2), 33.6 (C), 32.3 (CH_2), 29.7 (CH_3), 29.2 (CH_3), 25.3 (CH_2), 21.3 (2 × CH_2). HRMS (ESI): m/z calcd for $C_{16}H_{22}KO_4$ $[M+K]^+$ 317.1150, found 317.1146.

Dye-Sensitized Photooxygenation of 1. Compound **1** (300 mg, 1.46 mmol) and rose bengal (30 mg, 0.03 mmol) were dissolved in CCl_4 (150 mL), CH_3OH (10 mL), and CH_2Cl_2 (10 mL) before being irradiated with a 250 W halogen lamp under bubbling of oxygen for 1 h. The solvent was then removed under reduced pressure to afford a pink residue that was purified by column chromatography (SiO_2; hexanes/ethyl acetate, 9:1, v/v) to give **3** as a colorless solid (261 mg, 75% yield). Mp: 112.0−113.0 °C. IR (KBr): 3003, 2988, 2965, 2938, 1682, 1618, 1261, 1020 cm^{-1}. ^1H NMR (300 MHz, $CDCl_3$, 300 K, TMS): δ 7.52 (d, J = 6.0 Hz, 1H), 4.54 (d, J = 6.0 Hz, 1H), 2.33 (br s, 2H), 2.00−1.83 (AB system, J = 15.0 Hz, 2H), 1.57 (br s, 3H), 1.05 (br s, 3H), 1.02 (br s, 6H). ^{13}C NMR (75 MHz, $CDCl_3$, 300 K): δ 193.6 (C), 136.8 (C), 133.5 (CH), 97.9 (C), 76.2 (CH), 74.5 (C), 51.9 (CH_2), 43.0 (CH_2), 30.8 (C), 28.5 (2 × CH_3), 25.8 (CH_3), 24.9 (CH_3). HRMS (ESI) m/z calcd for $C_{13}H_{19}O_4$ $[M + H]^+$ 239.1278, found 239.1272.

■ ASSOCIATED CONTENT

Supporting Information

Compound characterization data, NMR spectra (1D ^1H, 1D ^{13}C, and 2D) of all products, *xyz* coordinates for computed structures, RDC and DP4 data analysis details, and complete ref 48. The Supporting Information is available free of charge on the ACS Publications website at DOI: 10.1021/acs.joc.5b00817.

■ AUTHOR INFORMATION

Corresponding Authors

*E-mail: mischne@iquir-conicet.gov.ar.

*E-mail: rgil@andrew.cmu.edu.

Notes

The authors declare no competing financial interest.

■ ACKNOWLEDGMENTS

We thank the Universidad Nacional de Rosario and Fundación Josefina Prats for financial support. M.J.R. thanks CONICET for fellowships. We also thank Dr. G. R. Labadie and Dr. C. M. J. Delpiccolo for HRMS measurements. A.N.-V. thanks the Universidade Federal de Pernambuco (UFPE) for a visiting professor contract. We thank the Galician Supercomputer Center (CESGA) for computer time allocation. NMR instrumentation at Carnegie Mellon University (CMU) was partially supported by the National Science Foundation (NSF) (Grants CHE-0130903 and CHE-1039870). R.R.G. acknowledges support from the NSF (Grant CHE-1111684).

■ REFERENCES

(1) Montagnon, T.; Tofi, M.; Vassilikogiannakis, G. *Acc. Chem. Res.* **2008**, *41*, 1001−1011.

(2) Buchanan, G. S.; Cole, K. P.; Tang, Y.; Hsung, R. P. *J. Org. Chem.* **2011**, *76*, 7027−7039.

(3) Peng, W.; Hirabaru, T.; Kawafuchi, H.; Inokuchi, T. *Eur. J. Org. Chem.* **2011**, *2011*, 5469−5474.

(4) Kepler, J. A.; Philip, A.; Lee, Y. W.; Morey, M. C.; Carroll, F. I. *J. Med. Chem.* **2002**, *31*, 713−716.

(5) Etoh, H.; Ina, K.; Iguichi, M. *Agric. Biol. Chem.* **1973**, *37*, 2241−2244.

(6) Huber, S.; Mischne, M. *Nat. Prod. Res.* **1995**, *7*, 43−46.

(7) Mischne, M. P.; Huber, S. N.; Zinczuk, J. *Can. J. Chem.* **1999**, *77*, 237−242.

(8) Borsarelli, C. D.; Mischne, M.; La Venia, A.; Moran Vieyra, F. E. *Photochem. Photobiol.* **2007**, *83*, 1313−1318.

(9) Coelho, P. J.; Carvalho, L. M.; Vermeersch, G.; Delbaere, S. *Tetrahedron* **2009**, *65*, 5369−5376.

(10) Huang, C.-N.; Kuo, P.-Y.; Lin, C.-H.; Yang, D.-Y. *Tetrahedron* **2007**, *63*, 10025−10033.

(11) Riveira, M. J.; Mischne, M. P. *Synth. Commun.* **2013**, *43*, 208−220.

(12) Bax, A.; Freeman, R.; Frenkiel, T. A. *J. Am. Chem. Soc.* **1981**, *103*, 2102−2104.

(13) Weigelt, J.; Otting, G. *J. Magn. Reson., Ser. A* **1995**, *113*, 128−130.

(14) Reif, B.; Köck, M.; Kerssebaum, R.; Kang, H.; Fenical, W.; Griesinger, C. *J. Magn. Reson., Ser. A* **1996**, *118*, 282−285.

(15) Reif, B.; Köck, M.; Kerssebaum, R.; Schleucher, J.; Griesinger, C. *J. Magn. Reson., Ser. A* **1996**, *112*, 295−301.

(16) Martin, G. E. *Annu. Rep. NMR Spectrosc.* **2011**, *74*, 215−291.

(17) Martin, G. E.; Reibarkh, M.; Buevich, A. V.; Blinov, K. A.; Williamson, R. T. *eMagRes* **2014**, *3*, 215−234.

DOI: 10.1021/acs.joc.5b00817
J. Org. Chem. 2015, 80, 7396−7402

(18) Blinov, K. A.; Larin, N. I.; Williams, A. J.; Mills, K. A.; Martin, G. E. *J. Heterocycl. Chem.* **2006**, *43*, 163−166.
(19) Snyder, D. A.; Brüschweiler, R. *J. Phys. Chem. A* **2009**, *113*, 12898−12903.
(20) ACD/Structure Elucidator Suite—Elucidate Unknown Structures. http://www.acdlabs.com/products/com_iden/elucidation/struc_eluc (accessed Feb 12, 2015).
(21) Rychnovsky, S. D. *Org. Lett.* **2006**, *13*, 2895−2898.
(22) Kummerlöwe, G.; Crone, B.; Kretschmer, M.; Kirsch, S. F.; Luy, B. *Angew. Chem., Int. Ed.* **2011**, *50*, 2643−2645.
(23) Gil, R. R.; Gayathri, C.; Tsarevsky, N. V.; Matyjaszewski, K. *J. Org. Chem.* **2008**, *73*, 840−848.
(24) Trigo-Mouriño, P.; Navarro-Vázquez, A.; Ying, J.; Gil, R. R.; Bax, A. *Angew. Chem., Int. Ed.* **2011**, *50*, 7576−7580.
(25) Thiele, C. M. *Concepts Magn. Reson., A* **2007**, *30A*, 65−80.
(26) Gayathri, C.; Tsarevsky, N. V.; Gil, R. R. *Chem.—Eur. J.* **2010**, *16*, 3622−3626.
(27) Freudenberger, J. C.; Spiteller, P.; Bauer, R.; Kessler, H.; Luy, B. *J. Am. Chem. Soc.* **2004**, *126*, 14690−14691.
(28) Aroulanda, C.; Sarfati, M.; Courtieu, J.; Lesot, P. *Enantiomer* **2001**, *6*, 281−287.
(29) Thiele, C. M.; Bermel, W. *J. Magn. Reson.* **2012**, *216*, 134−143.
(30) Furrer, J.; John, M.; Kessler, H.; Luy, B. *J. Biomol. NMR* **2007**, *37*, 231−243.
(31) Losonczi, J. A.; Andrec, M.; Fischer, M. W.; Prestegard, J. H. *J. Magn. Reson.* **1999**, *138*, 334−342.
(32) Navarro-Vázquez, A. *Magn. Reson. Chem.* **2012**, *50*, S73−S79.
(33) Thiele, C. M.; Schmidts, V.; Böttcher, B.; Louzao, I.; Berger, R.; Maliniak, A.; Stevensson, B. *Angew. Chem., Int. Ed.* **2009**, *48*, 6708−6712.
(34) Cornilescu, G.; Bax, A. *J. Am. Chem. Soc.* **2000**, *122*, 10143−10154.
(35) Smith, S. G.; Goodman, J. M. *J. Am. Chem. Soc.* **2010**, *132*, 12946−12959.
(36) Riveira, M. J.; Gayathri, C.; Navarro-Vázquez, A.; Tsarevsky, N. V.; Gil, R. R.; Mischne, M. P. *Org. Biomol. Chem.* **2011**, *9*, 3170−3175.
(37) Trigo-Mouriño, P.; Sifuentes, R.; Navarro-Vázquez, A.; Gayathri, C.; Maruenda, H.; Gil, R. R. *Nat. Prod. Commun.* **2012**, *7*, 735−738.
(38) Maheshwari, K. K.; de Mayo, P.; Wiegand, D. *Can. J. Chem.* **1970**, *48*, 3265−3268.
(39) Jeger, O.; Schaffner, K.; Wehrli, H. *Pure Appl. Chem.* **1964**, *9*, 555−566.
(40) Williams, J. R.; Sarkisian, G. M.; Quigley, J.; Hasiuk, A.; VanderVennen, R. *J. Org. Chem.* **1974**, *39*, 1028−1032.
(41) The source of water is unclear, and the same reaction side product was observed when using other dry solvents such as toluene or carbon tetrachloride.
(42) Singh, G. S.; Desta, Z. Y. *Chem. Rev.* **2012**, *112*, 6104−6155.
(43) Zheng, Y.; Tice, C. M.; Singh, S. B. *Bioorg. Med. Chem. Lett.* **2014**, *24*, 3673−3682.
(44) Valenta, P.; Drucker, N. A.; Bode, J. W.; Walsh, P. J. *Org. Lett.* **2009**, *11*, 2117−2119.
(45) Halgren, T. A. *J. Comput. Chem.* **1996**, *17*, 490−519.
(46) Halgren, T. A.; Nachbar, R. B. *J. Comput. Chem.* **1996**, *17*, 587−615.
(47) *Schrödinger Release 2014-1: MacroModel*, version 10.3; Schrödinger, LLC: New York, 2014.
(48) Frisch, M. J. et al. *Gaussian09*, revision D.01; Gaussian Inc.: Wallingford, CT, 2009.
(49) Zhang, Y.; Wu, A.; Xu, X.; Yan, Y. *Chem. Phys. Lett.* **2006**, *421*, 383−388.
(50) Tomasi, J.; Mennucci, B.; Cammi, R. *Chem. Rev.* **2005**, *105*, 2999−3093.
(51) Paier, J.; Hirschl, R.; Marsman, M.; Kresse, G. *J. Chem. Phys.* **2005**, *122*, 234102.
(52) Jensen, F. *J. Chem. Theory Comput.* **2008**, *4*, 719−727.

DOI: 10.1021/acs.joc.5b00817
J. Org. Chem. 2015, 80, 7396−7402